Commun. Theor. Phys. **77** (2025) 075401 (10pp)
https://doi.org/10.1088/1572-9494/ada9d5
CSTR: 32041.14.CTP.ada9d5

Shear viscoelasticity in anisotropic holographic axion model

Lei Li[1], **Wei-Jia Li**[1,*] **and Xiao-Mei Kuang**[2,*]

[1] Institute of Theoretical Physics, School of Physics, Dalian University of Technology, Dalian 116024, China
[2] Center for Gravitation and Cosmology, College of Physical Science and Technology, Yangzhou University, Yangzhou 225009, China

E-mail: weijiali@dlut.edu.cn and xmeikuang@yzu.edu.cn

Received 7 October 2024, revised 9 January 2025
Accepted for publication 13 January 2025
Published 27 March 2025

Abstract

In this work, we investigate the shear elasticity and the shear viscosity in a simple holographic axion model with broken translational symmetry and rotational symmetry in space via the perturbation computation. We find that, in the case of spontaneous symmetry breaking, the broken translations and anisotropy both enhance the shear elasticity of the system. While in all cases, the broken symmetries introduce a double suppression of the shear viscosity, which is in contrast to the result from the study of the p-wave holographic superfluid where the shear viscosity is enhanced when the rotational symmetry is broken spontaneously.

Keywords: gauge/gravity duality, holographic axion model, Black hole solution with perturbation

(Some figures may appear in colour only in the online journal)

1. Introduction

During the past two decades, the AdS/CFT correspondence has become a powerful tool for studying the real-time dynamics of strongly-coupled systems [1–4]. It provides us with a geometric approach to calculate transport coefficients of boundary systems explicitly in the AdS bulk by considering various black hole solutions that can dissipate the surrounding fluctuations outside their horizons. One of the most important discoveries of this method is that for a wide class of interacting systems, there exists a lower bound on the shear viscosity. And especially, for those having a gravity dual that can be described by Einstein gravity, the ratio of shear viscosity to entropy density η/s meets a universal value $\hbar/4\pi k_B$ which is called the Kovtun-Son-Starinet (KSS) bound [5–7]. Remarkably, such a finding in theory also explains why the ratio of shear viscosity to entropy density of the quark-gluon-plasma (QGP) is much smaller when compared to the result from the perturbative calculations of quantum field theory [8, 9]. This bound has been tested in various experiments of different realistic systems [10–14].

Nevertheless, it was found that η/s can be corrected when the finite N effect is considered. In this case, the viscosity bound can be slightly pushed down [15, 16].[3] In addition, the viscosity bound can be strongly violated when matter fields are included. Numerous specific examples have shown that this can happen when the rotational symmetry or the translational symmetry is broken (Examples of these two classes can be seen in [27–41] and [42–57], respectively.). In most of these cases, the way of breaking the symmetries is explicit. However, a recent holographic study on the p-wave superfluid model shows that the ratio η/s can be enhanced even in an anisotropic system if the rotations are broken in a spontaneous manner [58]. So far, this model appears to be the only known anisotropic case that obeys the KSS bound.

* Authors to whom any correspondence should be addressed.

[3] More generally, the violation of KSS bound was investigated in higher-order corrections [17–26].

In this work, we investigate the shear elasticity and the shear viscosity of an anisotropic holographic axion model at the perturbative level. This model allows us to realize the broken translations and the broken rotations explicitly and/or spontaneously via different setups. The boundary dual of this model is supposed to be certain viscoelastic strongly-coupled solids that exhibit both elastic responses as normal crystals and viscous damping as fluids. We expect that such a holographic tool will deepen our understanding of the viscoelastic properties of these complex materials in the real world. In particular, we would like to investigate the fate of the KSS bound in the case of spontaneous breaking of the symmetries. Our result shows that in contrast to the p-wave superfluid, the KSS bound is always violated in our model.

2. Anisotropic black hole solutions

We consider a simple holographic axion model [43, 48, 52, 59–62] in 4-dimensional spacetime, of which the action is given by

$$S = \int \mathrm{d}^4x\, \sqrt{-g}\left(R + \frac{6}{L^2} - \lambda^2\, V(X)\right),$$
$$X \equiv \frac{1}{2}\partial_\mu\phi^i\partial^\mu\phi^i, \quad i = x, y \tag{1}$$

where we have adopted the convention that $16\pi G \equiv 1$, R is the Ricci scalar, λ^2 is the effective coupling constant with the dimension of mass square,[4] V is a general function of X, and L is the AdS radius. To break the translations of the boundary system, the profiles of the scalars in the bulk should be chosen as

$$\phi^i = \mathcal{M}^i_j\, x^j, \qquad \mathcal{M}^i_j = \begin{pmatrix} k_x & 0 \\ 0 & k_y \end{pmatrix}. \tag{2}$$

Then, the general AdS black hole ansatz should be taken as

$$\begin{aligned} \mathrm{d}s^2 &= g_{tt}\mathrm{d}t^2 + g_{rr}\mathrm{d}r^2 + g_{xx}\mathrm{d}x^2 + g_{yy}\mathrm{d}y^2 \\ &= -A(r)\mathrm{d}t^2 + \frac{\mathrm{d}r^2}{A(r)} + B(r)\mathrm{d}x^2 + C(r)\mathrm{d}y^2 \end{aligned} \tag{3}$$

of which the metric components, at the AdS boundary $r \to \infty$, should satisfy

$$A(r \to \infty) = B(r \to \infty) = C(r \to \infty) = \frac{r^2}{L^2}. \tag{4}$$

The location of the horizon r_h is then defined by $A(r = r_h) = 0$. For simplicity, we will set L to be one,[5] and consider a class of specific models with

$$V(X) = X^n. \tag{5}$$

By considering $\phi^i = \bar{\phi}^i + \delta\phi^i$ and expanding the action to the second order in $\delta\phi^i$, we obtain

$$\frac{1}{2}V'(\bar{X})\partial_\mu\delta\phi^i\partial^\mu\delta\phi^i + \bar{X}V''(\bar{X})(\partial_i\delta\phi^i)^2 + \cdots. \tag{6}$$

[4] The physical coupling in front of $V(X)$, $\frac{\lambda^2}{16\pi G}$, should be dimensionless, which requires the dimension $[\lambda^2] = [G] = [M^2]$.

[5] This means that all the dimensional quantities are rescaled by L. For instance, $\lambda \to \lambda L$ which becomes a dimensionless quantity.

The absence of ghost requires monotonic potentials

$$V'(\bar{X}) > 0, \tag{7}$$

which gives us $n > 0$ [59]. For general $n > 0$, the axions behave like

$$\phi^i(r, x^\mu) = \phi^i_{(0)}(x^\mu) + \phi^i_{(1)}(x^\mu)\, r^{2n-5} + \cdots \tag{8}$$

near the AdS boundary, where the r-independent term corresponds to the profiles of the axions (2). Following the standard quantization, the leading mode of the axion fields sets the external source for the dual scalar operators on the boundary. The expectation values of the scalar operators correspond to the subleading mode of the axion fields. For $n < 5/2$, the r-independent term in (8) dominates over the expansion and plays the role of the external source. Then, the profile (2) with $k_x \neq k_y$ implies that the translations and the rotations are both broken explicitly. While, for $n > 5/2$, the r-independent term becomes subleading and the breaking of symmetries is spontaneous [63]. In the next section, we will investigate how the broken translations and the broken rotations affect the shear viscosity-entropy density ratio in these two scenarios.

In the following, we solve the background solutions perturbatively in two cases:

One-axion case

First, let us consider the single-axion case where $k_x = 0$, $k_y \neq 0$ are imposed without loss of generality. Note that the low anisotropic regime can be achieved by setting $\lambda \ll 1$ and fixing the value of k_y. Then, it is found that the background can be expressed perturbatively up to the leading order for $\mathcal{O}(\lambda^2)$,

$$A(r) = r^2\left(1 - \frac{r_h^3}{r^3}\right) + \lambda^2\, a_1^{(n)}(r) + \mathcal{O}(\lambda^4), \tag{9}$$

$$B(r) = r^2 + \lambda^2\, b_1^{(n)}(r) + \mathcal{O}(\lambda^4), \tag{10}$$

$$C(r) = r^2 - \lambda^2\, b_1^{(n)}(r) + \mathcal{O}(\lambda^4), \tag{11}$$

with

$$a_1^{(n)}(r) = \frac{k_y^{2n}}{2^{n+1}(2n-3)}\frac{r^{3-2n} - r_h^{3-2n}}{r}, \tag{12}$$

$$\begin{aligned} b_1^{(n)}(r) = \frac{n\, k_y^{2n}\, r^2\, r_h^{-2n}}{3\cdot 2^n\,(2n-3)}\Bigg[&\log\left(1 - \frac{r_h^3}{r^3}\right) \\ &+ \mathrm{Re}\,\mathcal{B}_0\left(\frac{r^3}{r_h^3}; 1 - \frac{2n}{3}, 0\right)\Bigg] + \gamma_{1(n)}\, r^2, \end{aligned} \tag{13}$$

where $\mathrm{Re}\mathcal{B}_0\left(x; 1 - \frac{2n}{3}, 0\right)$ represents the regular sector of the real part of the incomplete beta function $\mathcal{B}\left(x; 1 - \frac{2n}{3}, 0\right)$ and the constant $\gamma_{1(n)}$ is

$$\gamma_{1(n)} \equiv \begin{cases} \dfrac{n\,\pi\,k_y^{2n}\,r_h^{-2n}}{3\,(2n-3)\,2^n}\cot\left(\dfrac{2\pi n}{3}\right), & n \neq \dfrac{3}{2}z, \\ 0, & n = \dfrac{3}{2}(z+1), \end{cases} \tag{14}$$

with z denoting positive integers. Here, the special case $n = \frac{3}{2}$ has been excluded. It should be mentioned that the above results (12)–(14) are obtained by choosing the integral constants properly, which ensures the regularity of the background solution in the bulk and does not disrupt the asymptotic AdS geometry. For more details about the derivation, one refers to Appendix A. Then, the Hawking temperature can be read off as

$$T = \frac{A'(r_h)}{4\pi} = \frac{3\,r_h}{4\pi} - \lambda^2\,\frac{{k_y}^{2n}{r_h}^{1-2n}}{2^{n+3}\,\pi} + \mathcal{O}(\lambda^4). \tag{15}$$

While for $n = \frac{3}{2}$, one should solve it separately and obtain the corrections in the background metric as follows

$$a_1^{(n)}(r) = \frac{k_y^3}{4\sqrt{2}\,r}\log\left(\frac{r_h}{r}\right), \tag{16}$$

$$b_1^{(n)}(r) = -\frac{r^2\,k_y^3}{72\sqrt{2}\,r_h^3}\left[\pi^2 + 27\left(\log\frac{r}{r_h}\right)^2 + 6\,\mathrm{Li}_2\left(1 - \frac{r^3}{r_h^3}\right)\right], \tag{17}$$

with the polylogarithm function $\mathrm{Li}_2(x)$. And the Hawking temperature becomes

$$T = \frac{3\,r_h}{4\pi} - \lambda^2\frac{k_y^3}{16\,\sqrt{2}\,\pi\,r_h^2} + \mathcal{O}(\lambda^4). \tag{18}$$

2.1. Two-axion case

Now, we consider that there are two axions along both x and y directions, which means to set $k_x,\ k_y \neq 0$. For the general cases, one can assume that $k_x \neq k_y$. In the low anisotropic regime, we still have

$$A(r) = r^2\left(1 - \frac{r_h^3}{r^3}\right) + \lambda^2\,a_2^{(n)}(r) + \mathcal{O}(\lambda^4), \tag{19}$$

$$B(r) = r^2 + \lambda^2\,b_2^{(n)}(r) + \mathcal{O}(\lambda^4), \tag{20}$$

$$C(r) = r^2 - \lambda^2\,b_2^{(n)}(r) + \mathcal{O}(\lambda^4), \tag{21}$$

where

$$a_2^{(n)}(r) = \frac{(k_x^2+k_y^2)^n}{2^{n+1}(2n-3)}\frac{r^{3-2n} - r_h^{3-2n}}{r}, \tag{22}$$

$$b_2^{(n)}(r) = \frac{n\,(k_x^2+k_y^2)^{n-1}\,r^2\,r_h^{-2n}}{3\cdot 2^n\,(2n-3)}(k_y^2 - k_x^2) \times\left[\log\left(1 - \frac{r_h^3}{r^3}\right) + \mathrm{Re}\ \mathcal{B}_0\left(\frac{r^3}{r_h^3};\,1 - \frac{2n}{3},\,0\right)\right] + \gamma_{2(n)}\,r^2, \tag{23}$$

with

$$\gamma_{2(n)} \equiv \begin{cases} \dfrac{n\,\pi\,(k_y^2-k_x^2)\,(k_x^2+k_y^2)^{n-1}\,r_h^{-2n}}{3\,(2n-3)\,2^n}\cot\left(\dfrac{2\pi n}{3}\right), & n \neq \dfrac{3}{2}z, \\ 0, & n = \dfrac{3}{2}(z+1), \end{cases} \tag{24}$$

for $n \neq \frac{3}{2}$. The Hawking temperature then is given by

$$T = \frac{A'(r_h)}{4\pi} = \frac{3\,r_h}{4\pi} - \lambda^2\,\frac{(k_x^2+k_y^2)^n{r_h}^{1-2n}}{2^{n+3}\,\pi} + \mathcal{O}(\lambda^4). \tag{25}$$

For $n = \frac{3}{2}$, the results turn into

$$a_2^{(n)}(r) = \frac{(k_x^2+k_y^2)^{3/2}}{4\sqrt{2}\,r}\log\left(\frac{r_h}{r}\right), \tag{26}$$

$$b_2^{(n)}(r) = -\frac{r^2\,(k_y^2-k_x^2)\,\sqrt{k_x^2+k_y^2}}{72\sqrt{2}\,r_h^3} \times\left[\pi^2 + 27\left(\log\frac{r}{r_h}\right)^2 + 6\,\mathrm{Li}_2\left(1 - \frac{r^3}{r_h^3}\right)\right], \tag{27}$$

and

$$T = \frac{3\,r_h}{4\pi} - \lambda^2\,\frac{(k_x^2+k_y^2)^{3/2}}{16\,\sqrt{2}\,\pi\,r_h^2} + \mathcal{O}(\lambda^4). \tag{28}$$

In addition, one can easily check that, for the isotropic case (i.e., $k_x = k_y$), $b_2^{(n)}(r)$ is vanishing, which is consistent with the known results from previous studies on holographic solids [48, 52, 60, 62, 64].

3. Viscoelastic response

In the hydrodynamic limit (low frequency and small momentum), the retarded Green function of the stress tensor at zero momentum can be expanded as [65]

$$G^R_{T_{xy}T_{xy}}(\omega, \boldsymbol{p} = 0) = \mu_{xy} - \mathrm{i}\,\omega\,\eta_{xy} + \mathcal{O}(\omega^2), \tag{29}$$

where the non-dissipative part $\mu_{xy} = \lim_{\omega\to 0}\mathrm{Re}\ G^R_{T_{xy}T_{xy}}(\omega, \boldsymbol{p} = 0)$ is interpreted as the shear elastic modulus, and the dissipative coefficient η_{xy} in the imaginary part is associated to entropy production and should be understood as the shear viscosity.

In the holographic framework, to compute $G^R_{T_{xy}T_{xy}}(\omega, \boldsymbol{p} = 0)$, we need to introduce time-dependent perturbations δg_{xy} upon the background in the bulk. Note that this metric fluctuation is decoupled from other possible fluctuations for zero $\boldsymbol{p}$ because δg_{xy} is the solo fluctuation with the tensor channel in this sector. For $g_{ij} = \bar{g}_{ij} + \delta g_{ij}$ (From now on, we will use the bar to denote the background metric we obtained in the last section.), taking the Fourier

transformation $\delta g^i_j(t, r, x^i) \sim h^i_j(r)\, e^{-i\omega t}$, we achieve the equations of h^x_y and h^y_x as follows[6]:

$$\frac{1}{\sqrt{-g}}\partial_r(\sqrt{-g}\, Z_i{}^j(r)\bar{g}^{rr}\partial_r h^i_j) - \omega^2\bar{g}^{tt}Z_i{}^j(r)h^i_j = m^i_g(r)^2 Z_i{}^j(r)h^i_j, \quad (i = x, y \quad j = x, y). \tag{30}$$

where $Z_i{}^j(r) \equiv \bar{g}^{ij}\bar{g}_{ii}$ and the square of the graviton masses m_g^{i2} match the formula proposed in [47] which is given by

$$m_g^{i2} \equiv g^{ii}T_{ii} - \frac{\delta T_{ij}}{\delta g_{ij}}, \tag{31}$$

where the bulk stress tensor in our model is given by

$$T_{MN} = -g_{MN}\lambda^2\, V + \lambda^2\, V'(X)\, \partial_M\phi^i\partial_N\phi^i, \tag{32}$$

with $V' \equiv \frac{dV}{dX}$. Obviously, the graviton masses originate from the non-trivial profiles of the scalars in the bulk. For the isotropic case, i.e., $k_x = k_y = k$, we get $Z_i{}^j = 1$ and a unique graviton mass m_g. Then, the graviton behaves like a massive scalar in the bulk.

In our anisotropic model, there exist two distinct graviton masses which are

$$m_g^{i2} = \lambda^2\, k_i^2\, V'(\bar{X})\, \bar{g}^{ii}. \tag{33}$$

Therefore, the linearized perturbative equations of δg_{xy} can be expressed more explicitly as

$$\partial_r(\sqrt{-g}\, Z_i{}^j\bar{g}^{rr}\partial_r h^i_j) - \omega^2\sqrt{-g}\,\bar{g}^{tt}Z_i{}^j h^i_j = \lambda^2\, k_i^2\sqrt{-g}\,\bar{g}^{jj}V' h^i_j. \tag{34}$$

Next, we calculate the shear viscoelasticity both in the single-axion case and the two-axion case.

3.1. One-axion case

For $k_x = 0$, $k_y \neq 0$, the metric perturbation h^x_y satisfies the following equation

$$\partial_r(\sqrt{-g}\, Z^y_x\bar{g}^{rr}\partial_r h^x_y) - \omega^2\sqrt{-g}\, Z^y_x\bar{g}^{tt}h^x_y = 0. \tag{35}$$

Since the field is massless, one can apply the membrane paradigm which allows us to express the shear viscosity in terms of the horizon data [6, 17][7]. For the boundary system with two spatial dimensions, there can only be one shear viscosity η_{xy} and one shear modulus μ_{xy}. We will from now on omit the spatial indexes for simplicity. As a result, the shear viscosity to entropy density ratio can be expressed as

$$\frac{\eta}{s} = \frac{Z^y_x(r_h)}{4\pi} = \frac{1}{4\pi}\frac{\bar{g}_{xx}(r_h)}{\bar{g}_{yy}(r_h)} = \frac{1}{4\pi}\frac{B(r_h)}{C(r_h)}. \tag{36}$$

For the small λ, we obtain that

$$\frac{\eta}{s} = \frac{1}{4\pi} + \lambda^2\,\frac{b_1(r_h)}{2\,\pi\, {r_h}^2} + \mathcal{O}(\lambda^4). \tag{37}$$

In Appendix A, we have shown that $b_1(r_h) < 0$, which implies that, whether spontaneous or explicit, the rotational symmetry breaking always results in a violation of the KSS bound. In addition, the shear modulus in this case is zero due to the vanishing graviton mass.

Two-axion case

For $k_x,\ k_y \neq 0$, the rotational symmetry is entirely broken. In this case, h^x_y becomes massive which satisfies the following equation

$$\partial_r(\sqrt{-g}\, Z^y_x\bar{g}^{rr}\partial_r h^x_y) - \omega^2\sqrt{-g}\, Z^y_x\bar{g}^{tt}h^x_y = \lambda^2\, k_x^2\sqrt{-g}\,\bar{g}^{yy}V' h^x_y. \tag{38}$$

One can show that the graviton mass introduces a non-zero real part of $G^R_{T_{xy}T_{xy}}(\omega, \boldsymbol{p} = 0)$. Unlike the previous case, both μ and η now depend on the full geometry. The membrane paradigm is no longer applicable. However, for small λ, one can analytically calculate them order by order. The details are shown in Appendix B. As the result, μ and η/s are

$$\mu = \lambda^2\frac{n\, k_x^2\,(k_x^2 + k_y^2)^{n-1}}{2^{n-1}\,(2n-3)}r_h^{3-2n} + \mathcal{O}(\lambda^4), \quad n > \frac{3}{2} \tag{39}$$

and

$$\frac{\eta}{s} = \frac{1}{4\pi}\frac{B(r_h)}{C(r_h)} - \begin{cases} \lambda^2\dfrac{n\, k_x^2\,(k_x^2 + k_y^2)^{n-1}}{3\cdot 2^n\,(2n-3)\,\pi\, r_h^{2n}}\mathcal{H}(\dfrac{2n-3}{3}) + \mathcal{O}(\lambda^4), & n \neq \dfrac{3}{2}, \\ \lambda^2\dfrac{\pi\, k_x^2\sqrt{k_x^2 + k_y^2}}{72\sqrt{2}\, r_h^3} + \mathcal{O}(\lambda^4), & n = \dfrac{3}{2}, \end{cases} \tag{40}$$

where $\mathcal{H}(x)$ is harmonic number.

In order to separate the effects of broken translations and anisotropy in a manifest way, one can rotate the basis spatial coordinates as in [66],

$$\phi^i = k\begin{pmatrix} \sqrt{\frac{\epsilon^2}{4} + 1} & \frac{\epsilon}{2} \\ \frac{\epsilon}{2} & \sqrt{\frac{\epsilon^2}{4} + 1} \end{pmatrix}\begin{pmatrix} \tilde{x} \\ \tilde{y} \end{pmatrix}, \tag{41}$$

where k and ϵ are two dimensionless parameters characterizing the strengths of translational symmetry breaking and anisotropy, respectively. If we assume that $k_x > k_y$, then they are related to k and ϵ as follows,

$$k_x = k\left(\sqrt{\frac{\epsilon^2}{4} + 1} + \frac{\epsilon}{2}\right), \tag{42}$$

$$k_y = k\left(\sqrt{\frac{\epsilon^2}{4} + 1} - \frac{\epsilon}{2}\right). \tag{43}$$

[6] We here do not adopt the Einstein convention for the spatial indeces in the linearized equations.

[7] One can also obtain the shear viscosity by solving the equation of h^y_x whose mass makes the computation a little more difficult. However, as is shown in Appendix C the final result does not depend on which equation we solve.

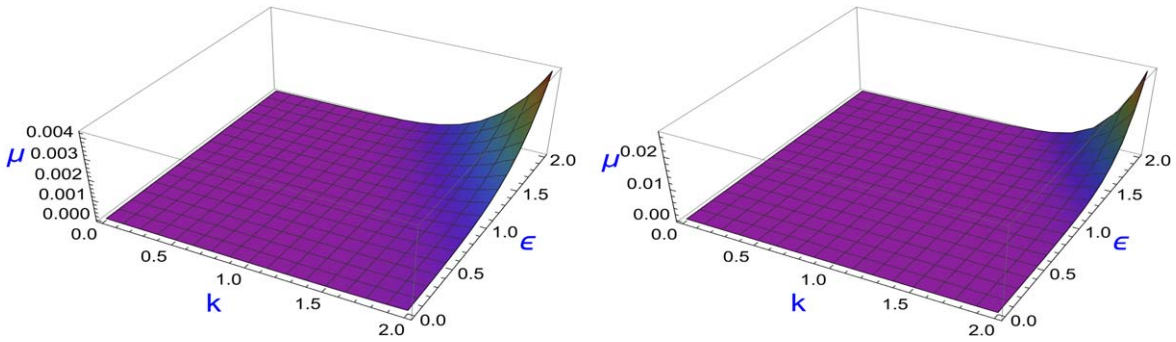

Figure 1. The shear modulus μ is the function of the k and ϵ, depicted by (44). Here, we have fixed $\lambda^2 L^2 = 10^{-5}$ and $r_h/L = 2$. **Left**: $n = 3$. **Right**: $n = 5$. In both cases, the symmetries are spontaneously broken.

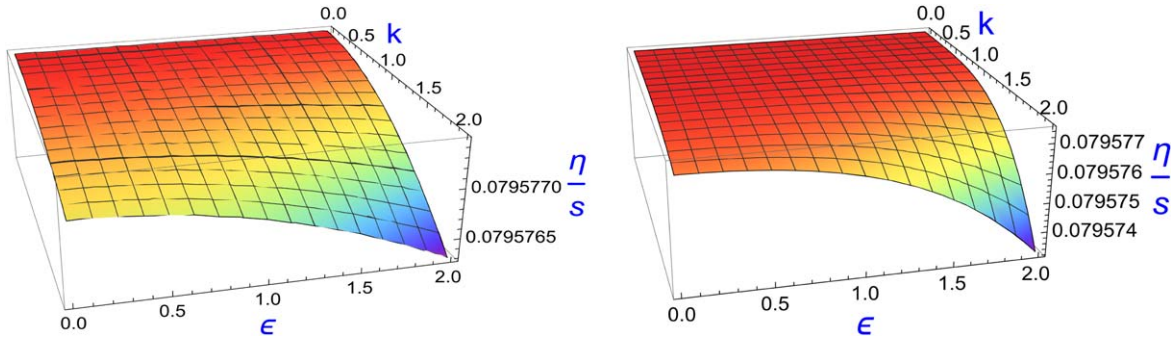

Figure 2. The ratio η/s as the function of the k and ϵ, depicted by (45). Here, we have fixed $\lambda^2 L^2 = 10^{-5}$ and $r_h/L = 2$. **Left**: $n = 1$. **Right**: $n = 2$. In both cases, the symmetries are explicitly broken.

Finally, (39) and (40) can be re-expressed as

$$\mu = \lambda^2 \frac{n\, k^{2n}\, (2+\epsilon^2)^{n-1}\, (\sqrt{4+\epsilon^2}+\epsilon)^2}{2^{n+1}\,(2n-3)\, r_h^{2n-3}} + \mathcal{O}(\lambda^4), \quad n > \frac{3}{2}, \tag{44}$$

and

$$\frac{\eta}{s} = \frac{1}{4\pi} - \begin{cases} \lambda^2 \frac{n\, k^{2n} (\epsilon^2+2)^n\, \mathcal{H}(\frac{2n-3}{3})}{3\cdot 2^{n+1}\,(2n-3)\,\pi\, r_h^{2n}} + \mathcal{O}(\lambda^4), & n \neq \frac{3}{2}, \\ \lambda^2 \frac{\pi\, [k^2(\epsilon^2+2)]^{3/2}}{144\,\sqrt{2}\, r_h^3} + \mathcal{O}(\lambda^4), & n = \frac{3}{2}. \end{cases} \tag{45}$$

From the above results, it is obvious to see that μ just increases monotonically with k and ϵ, and its value is enhanced faster for larger values of n. In Appendix A, we show that $\mathcal{H}(\frac{2n-3}{3}) < 0$ for $0 < n < \frac{3}{2}$ and $\mathcal{H}(\frac{2n-3}{3}) > 0$ for $n > \frac{3}{2}$. Therefore, η/s decreases monotonically with k and ϵ for all the cases. Furthermore, its value is suppressed more significantly for larger values of n, which implies that the KSS bound is always violated in the axion model, regardless of whether the symmetries are broken explicitly or spontaneously. In Figures 1–3, we plot μ and η/s as functions of k and ϵ for different cases.

4. Discussion and outlook

In this paper, the shear elasticity and the shear viscosity of an anisotropic holographic axion model with broken translations have been investigated. We find that a positive shear modulus emerges when the translational symmetry is broken spontaneously. In particular, the shear modulus is doubly enhanced in the presence of broken translations and anisotropy. Furthermore, the η/s ratio is always suppressed no matter whether the translations as well as the rotations are broken explicitly or spontaneously which is in contrast to the holographic p-wave superfluid case. In the p-wave superfluid, the spontaneous breaking of rotational symmetry caused by a vector condensate enhances the value of η/s, competing against the effects of explicit symmetry breaking. The KSS bound is hence never violated [58]. From this perspective, we can conclude that the fate of the KSS bound in holographic systems cannot be solely attributed to whether rotational symmetry is broken, or to the specific manner of that breaking (whether spontaneous or explicit). The η/s ratio also depends very much on the details of the operator that gives rise to the symmetry breaking.

In the case of the spontaneous symmetry breaking with $n > 5/2$, the holographic model is dual to a solid on the boundary. Then, one may naively expect that the violation of the viscosity bound cannot happen and that the shear viscosity should be divergent in a perfect crystal without topological defects, say, the dislocation flow. However, this does not contradict our results. We consider the frequency-dependent viscosity of the crystal given by the Kubo formula [67], $\eta^{\text{crystal}}(\omega) \equiv \text{Im}[G^R_{T_{xy}T_{xy}}(\omega, \boldsymbol{p}=0)/\omega] \approx \mu\, \delta(\omega) + \eta$, where the delta function is from the $1/\omega$ divergence of the real part

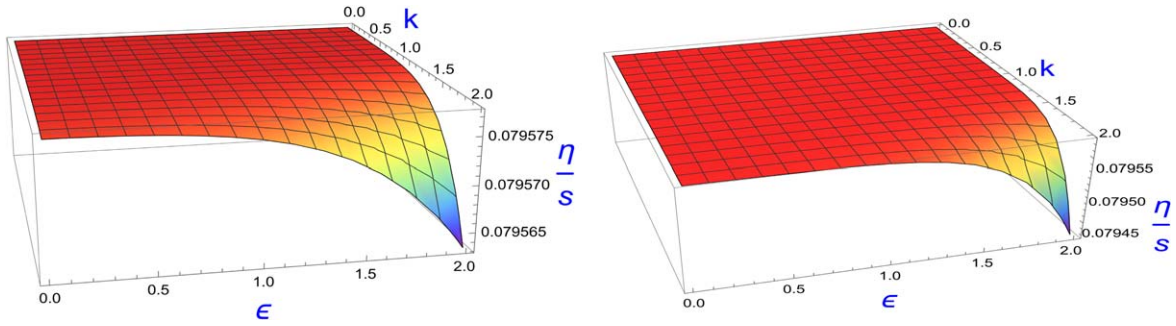

Figure 3. The ratio η/s as the function of the k and ϵ, depicted by (45). Here, we have fixed $\lambda^2 L^2 = 10^{-5}$ and $r_h/L = 2$. **Left**: $n = 3$. **Right**: $n = 5$. In both cases, the symmetries are spontaneously broken.

according to the Kramers–Kronig relation and η is the dissipative coefficient addressed in this work. In the DC limit, we have $\eta^{\text{crystal}} \to \infty$ due to the delta function. Therefore, although the KSS bound is violated, the crystal viscosity receives a divergent contribution from the rigidity of the translational order.

Nevertheless, our study in this work is limited to the perturbative region, i.e., the symmetry breaking is very weak. Therefore, it is not clear whether our conclusion holds or not when the breaking of the symmetries is finite. In a more general case, the anisotropic background solutions cannot be obtained in an analytic way. However, to achieve a complete answer, it is necessary to extend our study by, for instance, following the numeric methods used in [29, 30] to obtain the background solutions for finite values of λ and analyze how the viscoelastic property is affected in the strongly anisotropic region. We leave this for future work.

Acknowledgments

We would like to thank Matteo Baggioli, Kang Liu, Yan Liu, Ya-Wen Sun, and Ling-Zheng Xia for numerous helpful discussions. This work is supported by the National Natural Science Foundation of China (NSFC) under Grants Nos. 12275038 and 12375054.

Appendix A Corrections to the background solutions due to the axion fields

By the perturbative calculation, we can obtain the general solution of $a_1^{(n)}(r)$ as follows

$$a_1^{(n)}(r) = \frac{k_y^{2n}\, r^{2-2n}}{(2n-3)\, 2^{n+1}} - \frac{c_1}{r} + c_2, \tag{A1}$$

where c_1 and c_2 are integral constants which can be fixed as $c_1 = \frac{k_y^{2n}\, r_h^{3-2n}}{(2n-3)\, 2^{n+1}}$ and $c_2 = 0$ so that $a_1^{(n)}(r)$ is regular at the horizon and does not destroy the asymptotic AdS.

The general solution of $b_1^{(n)}(r)$ is

$$b_1^{(n)}(r) = \frac{1}{3} r^2 \left[\frac{n\, k_y^{2n}\, \mathcal{B}\left(\frac{r^3}{r_h^3}; 1 - \frac{2n}{3}, 0\right)}{(2n-3)\, 2^n\, r_h^{2n}} + \frac{c_3 \log\left(1 - \frac{r_h^3}{r^3}\right)}{r_h^3} + 3\, c_4 \right], \tag{A2}$$

with integral constants c_3 and c_4, the incomplete beta function $\mathcal{B}\left(\frac{r^3}{r_h^3}, 1 - \frac{2n}{3}, 0\right)$ which is logarithmically divergent at the horizon. Then, we have to choose $c_3 = \frac{n\, k_y^{2n}\, r_h^{3-2n}}{(2n-3)\, 2^n}$ so that the logarithmic divergence $\mathcal{B}$ can be canceled. In addition, $\mathcal{B}$ is complex, but when $n \neq \frac{3}{2}\mathbb{Z}$ and $r > r_h$, its imaginary part is independent of r. Then, we can choose c_4 properly to remove the imaginary part of $\mathcal{B}$. On the other hand, since $\text{Re}\, \mathcal{B}\left(\infty; 1 - \frac{2n}{3}, 0\right) = -\pi \cot\left(\frac{2\pi n}{3}\right)$, we have to fix

$$c_4 = \frac{n\, \pi\, k_y^{2n}\, r_h^{-2n}}{3\,(2n-3)\, 2^n} \cot\left(\frac{2\pi n}{3}\right) - \frac{n\, k_y^{2n}}{3\,(2n-3)\, 2^n\, r_h^{2n}} \times \text{Im}\, \mathcal{B}\left(\frac{r^3}{r_h^3}; 1 - \frac{2n}{3}, 0\right), \tag{A3}$$

so that the boundary is still AdS. However, when $n = \frac{3}{2}(\mathbb{Z} + 1)$ and $r > r_h$, the real part of $\mathcal{B}$ becomes divergent. Then, we have to choose c_4 properly so that Im $\mathcal{B}$ and the divergence of Re $\mathcal{B}$ are both removed. In this case, only the regular part of $\mathcal{B}$ (which we denoted as $\mathcal{B}_0$ in the main text) is left. One can further check that $\text{Re}\, \mathcal{B}_0\left(\infty; 1 - \frac{2n}{3}, 0\right) = 0$. Then, in all the cases (except for $n = \frac{3}{2}$), we obtain the result (13) in the main text.

At the horizon, we obtain that

$$b_1^{(n)}(r_h) = \begin{cases} \frac{n\, k_y^{2n}\, r_h^{2-2n}}{3 \cdot 2^n\, (3-2n)} \mathcal{H}\left(\frac{2n-3}{3}\right), & n \neq \frac{3}{2}, \\ -\frac{\pi^2 k_y^3}{72\sqrt{2}\, r_h}, & n = \frac{3}{2}. \end{cases} \tag{A4}$$

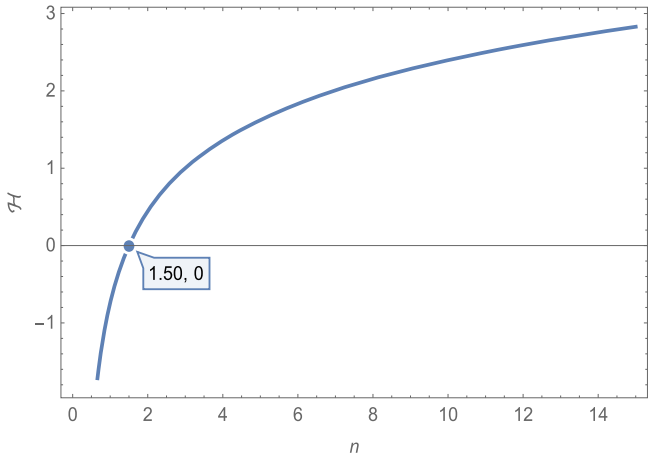

Figure 4. $\mathcal{H}(\frac{2n-3}{3})$ as the function of n.

In Figure 4, we plot $\mathcal{H}(\frac{2n-3}{3})$ as the function of n. When $0 < n < \frac{3}{2}$, we have $\mathcal{H}(\frac{2n-3}{3}) < 0$. In contrast, when $n > \frac{3}{2}$, we find that $\mathcal{H}(\frac{2n-3}{3}) > 0$. Then, we conclude that $b_1^{(n)}(r_h)$ is always negative in the one-axion case.

Repeating the calculation, in the two-axion case, we have that

$$b_2^{(n)}(r_h) = \begin{cases} \dfrac{n\, r_h^{2-2n}(k_y^2 - k_x^2)\,(k_x^2 + k_y^2)^{n-1}}{3 \cdot 2^n\,(3-2n)}\mathcal{H}(\dfrac{2n-3}{3}), & n \neq \dfrac{3}{2}, \\ -\dfrac{\pi^2(k_y^2 - k_x^2)\sqrt{k_x^2 + k_y^2}}{72\sqrt{2}\, r_h}, & n = \dfrac{3}{2}. \end{cases} \tag{A5}$$

Inserting the result above into (40) in the main text, we immediately obtain the result (45).

Appendix B Derivation of the shear viscoelasticity for the two-axion case

We consider the two-axion case and take the fluctuating metric h_y^x for example and denote it as h for simplicity. Recall that it satisfies

$$h'' + \left(\frac{A'}{A} + \frac{3B'}{2B} - \frac{C'}{2C}\right)h' + \left(\frac{\omega^2}{A^2} - \frac{m_g^2}{A}\right)h = 0,$$
$$m_g^2 = \frac{\lambda^2 k_x^2 V'}{B}, \tag{B1}$$

where h' denotes the derivative of h with respect to r.

To compute the Green function of the stress tensor, we look for a special solution to the equation that is normalized to be a unit at the AdS boundary. Suppose that the solution near the boundary behaves like

$$h = (1 + \cdots) + h_3(\omega)\, r^{-3}(1 + \cdots). \tag{B2}$$

The Green function of the stress tensor can be read off as

$$G^R_{T_{xy}T_{xy}}(\omega, \boldsymbol{p} = 0) = -3\, h_3(\omega). \tag{B3}$$

To extract η and μ, we need to solve (B1) up to $\mathcal{O}(\omega)$ by taking the low-frequency expansion. In addition, we require the solution to satisfy the infalling boundary condition at the horizon. We hence take the following ansatz that

$$h(r) = f(r)^{-i\omega/4\pi T}\Big[H_0^{(0)}(r) + \lambda^2\, H_0^{(2)}(r) + \frac{i\omega}{4\pi T} \times (H_1^{(0)}(r) + \lambda^2\, H_1^{(2)}(r)) + \mathcal{O}(\omega^2)\Big]. \tag{B4}$$

where $f(r) \equiv A(r)/r^2$. $H_0^{(0)}(r)$, $H_0^{(2)}(r)$, $H_1^{(0)}(r)$, and $H_1^{(2)}(r)$ should be regular functions in the bulk including the horizon. The upper index of $H(r)$ denotes the order of λ and the lower index of $H(r)$ denotes the order of ω.

Firstly, let us calculate the zeroth order (i.e., $m_g^2 = 0$). Plugging (B4) into (B1), we obtain the following two equations

$$0 = H_0^{(0)\prime\prime} + \left(\frac{f'}{f} + \frac{2}{r} + \frac{3B'}{2B} - \frac{C'}{2C}\right)H_0^{(0)\prime}, \tag{B5}$$

$$0 = H_1^{(0)\prime}\left(\frac{f'}{f} + \frac{2}{r} + \frac{3B'}{2B} - \frac{C'}{2C}\right) + H_1^{(0)\prime\prime} - H_0^{(0)\prime}\frac{2f'}{f} - H_0^{(0)}\left[\left(\frac{2}{r} + \frac{3B'}{2B} - \frac{C'}{2C}\right)\frac{f'}{f} + \frac{f''}{f}\right]. \tag{B6}$$

The regular solution to (B5) that meets the asymptotic behavior (B2) is given by

$$H_0^{(0)} = 1. \tag{B7}$$

With this, $H_1^{(0)}(r)$ can be further determined by (B6) and (B2), which is

$$H_1^{(0)}(r) = c_6 + \int_{r_h}^{r} dy \frac{f'(y)}{f(y)} + c_5 \int_{r_h}^{r} dy \frac{C(y)^{1/2}}{A(y)B(y)^{3/2}}. \tag{B8}$$

Combining the regularity of $H_1^{(0)}$ at the horizon and analyzing its asymptotic behavior, one can obtain that $c_5 = -\frac{A'(r_h)B(r_h)^{3/2}}{C(r_h)^{1/2}}$ and $c_6 = 0$. Then, near the boundary($r \to \infty$), we find that

$$H_1^{(0)}(r) = \frac{1}{3r^3}\frac{A'(r_h)B(r_h)^{3/2}}{C(r_h)^{1/2}} + \cdots, \tag{B9}$$

$$h(r) = 1 + \frac{i\omega B(r_h)^{3/2}C(r_h)^{-1/2}}{3r^3} + \cdots. \tag{B10}$$

Using the holographic dictionary, the retarded Green function can be read off as

$$G^R_{T_{xy}T_{xy}}(\omega, \boldsymbol{p} = 0) = -i\omega\, B(r_h)^{3/2}C(r_h)^{-1/2} \equiv -i\omega\eta, \tag{B11}$$

which is purely imaginary. Since the entropy density $s = 4\,\pi\sqrt{BC}|_{r=r_h}$, the viscosity to entropy density ratio should be

$$\frac{\eta}{s} = \frac{1}{4\pi}\frac{B(r_h)}{C(r_h)}. \tag{B12}$$

If the system has an $SO(2)$ symmetry on the $x - y$ plane, i.e, $B(r) = C(r)$, it reduces to the celebrated KSS bound.

Now, we turn to the order $\mathcal{O}(\lambda^2)$ by setting $m_g^2(r) \equiv \lambda^2\, M^2(r)$ with $M^2(r) = \frac{k_x^2 V'}{B}$. Subsequently, we

have two equations

$$0 = H_0^{(2)\prime\prime} + \left(\frac{f'}{f} + \frac{2}{r} + \frac{3B'}{2B} - \frac{C'}{2C}\right)H_0^{(2)\prime} - \frac{M^2}{r^2 f}H_0^{(0)}, \tag{B13}$$

$$\begin{aligned} 0 = {} & H_1^{(2)\prime}\left(\frac{f'}{f} + \frac{2}{r} + \frac{3B'}{2B} - \frac{C'}{2C}\right) \\ & + H_1^{(2)\prime\prime} - H_1^{(0)}\frac{M^2}{r^2 f} - H_0^{(2)\prime}\frac{2f'}{f} \\ & - H_0^{(2)}\left[\left(\frac{2}{r} + \frac{3B'}{2B} - \frac{C'}{2C}\right)\frac{f'}{f} + \frac{f''}{f}\right]. \end{aligned} \tag{B14}$$

We just simply replace the background appearing in order $\mathcal{O}(\lambda^2)$ with the Schwarzschild metric. We find that the third and last terms in (B14) vanish on the Schwarzschild background[8]. In this way, we obtain that

$$\begin{aligned} H_0^{(2)}(r) = {} & c_8 + c_7\int_{r_h}^{r} \mathrm{d}x \frac{C(x)^{1/2}}{A(x)B(x)^{3/2}} \\ & + \int_{r_h}^{r} \mathrm{d}x\left(\frac{C(x)^{1/2}}{A(x)B(x)^{3/2}}\int_{r_h}^{x} \mathrm{d}y \frac{B(y)^{3/2}H_0^{(0)}(y)}{C(y)^{1/2}}M^2(y)\right), \end{aligned} \tag{B15}$$

$$\begin{aligned} H_1^{(2)}(r) = {} & c_{10} + c_9\int_{r_h}^{r} \mathrm{d}x \frac{C(x)^{1/2}}{A(x)B(x)^{3/2}} \\ & + \int_{r_h}^{r} \mathrm{d}x\left(\frac{C(x)^{1/2}}{A(x)B(x)^{3/2}}\int_{r_h}^{x} \mathrm{d}y \frac{2y^2 B(y)^{3/2}f'(y)}{C(y)^{1/2}}H_0^{(2)\prime}(y)\right). \end{aligned} \tag{B16}$$

B.0.1. $n \neq \frac{3}{2}$

Using (B7) and $M^2(y) = \frac{k_x^2 V'}{B(y)} = \frac{n\,k_x^2}{y^2}\left(\frac{k_x^2}{2\,y^2} + \frac{k_y^2}{2\,y^2}\right)^{n-1}$, we obtain

$$\begin{aligned} H_0^{(2)}(r) = {} & \int_{r_h}^{r} \mathrm{d}x\left[\frac{C(x)^{1/2}}{A(x)B(x)^{3/2}}\int_{r_h}^{x} \mathrm{d}y \frac{n\,y^{2-2n}\,k_x^2(k_x^2+k_y^2)^{n-1}}{2^{n-1}}\right] \\ = {} & N\int_{r_h}^{r} \mathrm{d}x \frac{x^{3-2n}}{x^4(1-\frac{r_h^3}{x^3})} \\ & - N\,r_h^{3-2n}\int_{r_h}^{r} \mathrm{d}x \frac{1}{x^4(1-\frac{r_h^3}{x^3})}, \quad n \neq \frac{3}{2}, \end{aligned} \tag{B17}$$

where $N \equiv \frac{n\,k_x^2(k_x^2+k_y^2)^{n-1}}{2^{n-1}(3-2n)}$. The two conditions of regular function and asymptotic behavior near the boundary require the integral constants c_7 and c_8 to be zero. Then,

$$H_0^{(2)\prime}(r) = N\frac{r^{3-2n}}{r^4(1-\frac{r_h^3}{r^3})} - N\frac{r_h^{3-2n}}{r^4(1-\frac{r_h^3}{r^3})}. \tag{B18}$$

Near the boundary ($r \to \infty$),

$$H_0^{(2)}(r) = -\frac{1}{3r^3}\frac{nk_x^2(k_x^2+k_y^2)^{n-1}}{2^{n-1}(2n-3)}r_h^{3-2n} + \cdots. \tag{B19}$$

[8] It is found that $H_1^{(0)}$ is zero when we just bring the Schwarzschild metric into (B8).

Combining (B16) and (B18), we have

$$\begin{aligned} H_1^{(2)}(r) = {} & c_{10} + c_9\int_{r_h}^{r} \mathrm{d}x \frac{C(x)^{1/2}}{A(x)B(x)^{3/2}} \\ & + 6\,N\,r_h^3\int_{r_h}^{r} \mathrm{d}x\left[\frac{C(x)^{1/2}}{A(x)B(x)^{3/2}}(F(x) \right. \\ & \left. - F(r_h))\right] - 6\,N\,r_h^{6-2n}\int_{r_h}^{r} \mathrm{d}x\left[\frac{C(x)^{1/2}}{A(x)B(x)^{3/2}} \right. \\ & \left. \times (G(x) - G(r_h))\right], \end{aligned} \tag{B20}$$

where

$$\begin{aligned} F(x) - F(r_h) = {} & -\frac{1}{3}r_h^{-2n}\left[\mathcal{B}\left(\frac{y^3}{r_h^3}, 1-\frac{2n}{3}, 0\right)\right]|_{y=r_h}^{y=x}, \\ G(x) - G(r_h) = {} & \frac{1}{3\,r_h^3}\left[\log\left(\frac{y^3-r_h^3}{y^3}\right)\right]|_{y=r_h}^{y=x}, \end{aligned} \tag{B21}$$

with the incomplete beta function $\mathcal{B}\left(\frac{y^3}{r_h^3}, 1-\frac{2n}{3}, 0\right)$. We need to fix the integral constants $c_9 = c_{10} = 0$ so that $H_1^{(2)}(r)$ ensures the regularity of the solution at the horizon and the asymptotic behavior (B2) near the boundary. Then, near the boundary, we take the expansion of $A(x)$, $B(x)$, $C(x)$, $F(x)$, $G(x)$ and insert them into (B20). We immediately get

$$H_1^{(2)}(r) = -\frac{1}{3r^3}\frac{nk_x^2(k_x^2+k_y^2)^{n-1}}{2^{n-2}(2n-3)\,r_h^{2n-3}}\,\mathcal{H}\left(\frac{2n-3}{3}\right) + \cdots. \tag{B22}$$

In the end, for $V(X) = X^n$ model, substituting (B7), (B9), (B19) and (B22) into (B4), we derive that

$$\mu = \lambda^2\frac{n\,k_x^2\,(k_x^2+k_y^2)^{n-1}}{2^{n-1}\,(2n-3)}r_h^{3-2n} + \mathcal{O}(\lambda^4), \quad n > \frac{3}{2}, \tag{B23}$$

$$\begin{aligned} \frac{\eta}{s} = {} & \frac{1}{4\pi}\frac{B(r_h)}{C(r_h)} - \lambda^2\frac{n\,k_x^2\,(k_x^2+k_y^2)^{n-1}}{3\cdot 2^n\,(2n-3)\,\pi\,r_h^{2n}} \\ & \times \mathcal{H}(\frac{2n-3}{3}) + \mathcal{O}(\lambda^4). \end{aligned} \tag{B24}$$

B.0.2. $n = \frac{3}{2}$

In this case, $M^2(y) = \frac{k_x^2 V'}{B(y)} = \frac{3\,k_x^2}{2\,y^2}\left(\frac{k_x^2}{2\,y^2} + \frac{k_y^2}{2\,y^2}\right)^{1/2}$, we have

$$H_0^{(2)}(r) = \frac{3\,k_x^2\sqrt{k_x^2+k_y^2}}{2\sqrt{2}}\int_{r_h}^{r} \mathrm{d}x \frac{\log(\frac{x}{r_h})}{x^4(1-\frac{r_h^3}{x^3})}, \tag{B25}$$

where c_7 and c_8 are also zero. Then,

$$H_0^{(2)\prime}(r) = \frac{3\,k_x^2\sqrt{k_x^2+k_y^2}}{2\sqrt{2}}\frac{\log(\frac{r}{r_h})}{r^4(1-\frac{r_h^3}{r^3})}. \tag{B26}$$

Near the boundary ($r \to \infty$),

$$H_0^{(2)}(r) = -\frac{1}{r^3}\frac{k_x^2\sqrt{k_x^2+k_y^2}}{6\sqrt{2}} + \frac{1}{r^3}\log\left(\frac{r_h}{r}\right)\frac{k_x^2\sqrt{k_x^2+k_y^2}}{2\sqrt{2}} + \cdots, \tag{B27}$$

where $\log\left(\frac{r_h}{r}\right)$ is divergent at the boundary.

Combining (B16) and (B26), near the boundary, the regular function $H_1^{(2)}(r)$ is obtained by repeating the calculation

$$H_1^{(2)}(r) = -\frac{1}{r^3}\frac{\pi^2\, k_x^2\sqrt{k_x^2+k_y^2}}{18\sqrt{2}} + \cdots, \tag{B28}$$

where we have chosen $c_9 = c_{10} = 0$ so that $H_1^{(2)}(r)$ ensures the regularity at the horizon and the asymptotic behavior (B2) near the boundary. Finally, for $V(X) = X^{\frac{3}{2}}$ model, we find that

$$\frac{\eta}{s} = \frac{1}{4\pi}\frac{B(r_h)}{C(r_h)} - \lambda^2\frac{\pi\, k_x^2\sqrt{k_x^2+k_y^2}}{72\sqrt{2}\, r_h^3} + \mathcal{O}(\lambda^4). \tag{B29}$$

Appendix C Shear viscosity calculated by the eom of h_x^y

In the section on the one-axion case in the main text, we mentioned that the result of the shear viscosity does not depend on whether solving the eom of h_y^x or the one of h_x^y. Here, we will show that solving the equation of the massive h_x^y also gives the result (37). Analogous to the calculations in Appendix B, we have the following formula for the massive field

$$\frac{\eta}{s} = \frac{1}{4\pi}\frac{C(r_h)}{B(r_h)} - \begin{cases} \lambda^2\frac{n\, k^{2n}\,\mathcal{H}(\frac{2n-3}{3})}{3\cdot 2^n\,(2n-3)\,\pi\, r_h^{2n}} + \mathcal{O}(\lambda^4), & n \neq \frac{3}{2}, \\ \lambda^2\frac{\pi\, k^3}{72\sqrt{2}\, r_h^3} + \mathcal{O}(\lambda^4), & n = \frac{3}{2}, \end{cases} \tag{C1}$$

which is obtained by setting $k_x = 0$ and $k_y = k \neq 0$. This seems very different from the result we achieved in the main text, but expanding

$$\frac{C(r_h)}{B(r_h)} = 1 - \lambda^2\frac{2\, b_1^{(n)}(r_h)}{r_h^2} + \mathcal{O}(\lambda^4) \tag{C2}$$

and combining it with (A4) directly gives us

$$\frac{\eta}{s} = \frac{1}{4\pi} + \lambda^2\frac{b_1^{(n)}(r_h)}{2\,\pi\, {r_h}^2} + \mathcal{O}(\lambda^4), \tag{C3}$$

which is exactly the result (37).

References

[1] Ammon M and Erdmenger J 2015 *Gauge/Gravity Duality: Foundations and Applications* (Cambridge: Cambridge University Press)

[2] Zaanen J, Liu Y, Sun Y-W and Schalm K 2015 *Holographic Duality in Condensed Matter Physics* (Cambridge: Cambridge University Press)

[3] Hartnoll S A, Lucas A and Sachdev S 2018 *Holographic Quantum Matter* (Cambridge, MA: MIT Press)

[4] Baggioli M 2019 *Applied Holography: A Practical Mini-Course* (*Springer Briefs in Physics*) (Berlin: Springer)

[5] Policastro G, Son D T and Starinets A O 2001 The shear viscosity of strongly coupled N=4 supersymmetric Yang–Mills plasma *Phys. Rev. Lett.* **87** 081601

[6] Kovtun P, Son D T and Starinets A O 2003 Holography and hydrodynamics: diffusion on stretched horizons *J. High Energy Phys.* JHEP10(2003)064

[7] Kovtun P, Son D T and Starinets A O 2005 Viscosity in strongly interacting quantum field theories from black hole physics *Phys. Rev. Lett.* **94** 111601

[8] Arnold P B, Moore G D and Yaffe L G 2003 Transport coefficients in high temperature gauge theories. 2. Beyond leading log *J. High Energy Phys.* JHEP05(2003)051

[9] Huot S C, Jeon S and Moore G D 2007 Shear viscosity in weakly coupled $N = 4$ super Yang–Mills theory compared to QCD *Phys. Rev. Lett.* **98** 172303

[10] Luzum M and Romatschke P 2008 Conformal relativistic viscous hydrodynamics: applications to RHIC results at s_{NN} = 200 GeV *Phys. Rev.* C **78** 034915
Erratum: 2009 *Phys. Rev.* C **79** 039903

[11] Schäfer T and Teaney D 2009 Nearly perfect fluidity: from cold atomic gases to hot quark gluon plasmas *Rept. Prog. Phys.* **72** 126001

[12] Cremonini S 2011 The shear viscosity to entropy ratio: a status report *Mod. Phys. Lett.* B **25** 1867–88

[13] Nagle J L, Bearden I G and Zajc W A 2011 Quark-gluon plasma at RHIC and the LHC: perfect fluid too perfect? *New J. Phys.* **13** 075004

[14] Shen C, Heinz U, Huovinen P and Song H 2011 Radial and elliptic flow in Pb+Pb collisions at the CERN Large Hadron Collider from viscous hydrodynamic *Phys. Rev.* C **84** 044903

[15] Brigante M, Liu H, Myers R C, Shenker S and Yaida S 2008 The viscosity bound and causality violation *Phys. Rev. Lett.* **100** 191601

[16] Brigante M, Liu H, Myers R C, Shenker S and Yaida S 2008 Viscosity bound violation in higher derivative gravity *Phys. Rev.* D **77** 126006

[17] Iqbal N and Liu H 2009 Universality of the hydrodynamic limit in AdS/CFT and the membrane paradigm *Phys. Rev.* D **79** 025023

[18] Cai R-G, Nie Z-Y and Sun Y-W 2008 Shear viscosity from effective couplings of gravitons *Phys. Rev.* D **78** 126007

[19] Cai R-G and Sun Y-W 2008 Shear viscosity from AdS Born–Infeld black holes *J. High Energy Phys.* JHEP09(2008)115

[20] Brustein R and Medved A J M 2009 The ratio of shear viscosity to entropy density in generalized theories of gravity *Phys. Rev.* D **79** 021901

[21] Cai R-G, Nie Z-Y, Ohta N and Sun Y-W 2009 Shear viscosity from Gauss–Bonnet gravity with a dilaton coupling *Phys. Rev.* D **79** 066004

[22] Kats Y and Petrov P 2009 Effect of curvature squared corrections in AdS on the viscosity of the dual gauge theory *J. High Energy Phys.* JHEP01(2009)044

[23] Myers R C, Paulos M F and Sinha A 2010 Holographic studies of quasi-topological gravity *J. High Energy Phys.* JHEP08 (2010)035

[24] Feng X-H, Liu H-S, Lü H and Pope C N 2015 Black hole entropy and viscosity bound in Horndeski gravity *J. High Energy Phys.* JHEP11(2015)176

[25] Wang Y-L and Ge X-H 2016 Shear viscosity to entropy density ratio in higher derivative gravity with momentum dissipation *Phys. Rev.* D **94** 066007

[26] Buchel A 2024 Holographic Gauss–Bonnet transport *Phys. Lett.* B **853** 138666

[27] Natsuume M and Ohta M 2010 The shear viscosity of holographic superfluids *Prog. Theor. Phys.* **124** 931–51

[28] Erdmenger J, Kerner P and Zeller H 2011 Non-universal shear viscosity from Einstein gravity *Phys. Lett.* B **699** 301–4

[29] Rebhan A and Steineder D 2012 Violation of the holographic viscosity bound in a strongly coupled anisotropic plasma *Phys. Rev. Lett.* **108** 021601

[30] Mamo K A 2012 Holographic RG flow of the shear viscosity to entropy density ratio in strongly coupled anisotropic plasma *J. High Energy Phys.* JHEP10(2012)070

[31] Giataganas D 2013 Observables in strongly coupled anisotropic theories *PoS Corfu.* **2012** 122

[32] Jain S, Kundu N, Sen K, Sinha A and Trivedi S P 2015 A strongly coupled anisotropic fluid from dilaton driven holography *J. High Energy Phys.* JHEP01(2015)005

[33] Critelli R, Finazzo S I, Zaniboni M and Noronha J 2014 Anisotropic shear viscosity of a strongly coupled non-Abelian plasma from magnetic branes *Phys. Rev.* D **90** 066006

[34] Ge X-H, Ling Y, Niu C and Sin S-J 2015 Thermoelectric conductivities, shear viscosity, and stability in an anisotropic linear axion model *Phys. Rev.* D **92** 106005

[35] Jain S, Samanta R and Trivedi S P 2015 The shear viscosity in anisotropic phases *J. High Energy Phys.* JHEP10(2015)028

[36] Ge X-H 2016 Notes on shear viscosity bound violation in anisotropic models *Sci. China Phys. Mech. Astron.* **59** 630401

[37] Landsteiner K, Liu Y and Sun Y-W 2016 Odd viscosity in the quantum critical region of a holographic Weyl semimetal *Phys. Rev. Lett.* **117** 081604

[38] Finazzo S I, Critelli R, Rougemont R and Noronha J 2016 Momentum transport in strongly coupled anisotropic plasmas in the presence of strong magnetic fields *Phys. Rev.* D **94** 054020

[39] Samanta R, Sharma R and Trivedi S P 2017 Shear viscosity in an anisotropic unitary Fermi gas *Phys. Rev.* A **96** 053601

[40] Jeong H-S, Ahn Y, Ahn D, Niu C, Li W-J and Kim K-Y 2018 Thermal diffusivity and butterfly velocity in anisotropic Q-lattice models *J. High Energy Phys.* JHEP01(2018)140

[41] Giataganas D, Gürsoy U and Pedraza J F 2018 Strongly-coupled anisotropic gauge theories and holography *Phys. Rev. Lett.* **121** 121601

[42] Davison R A and Goutéraux B 2015 Momentum dissipation and effective theories of coherent and incoherent transport *J. High Energy Phys.* JHEP01(2015)039

[43] Baggioli M 2016 Gravity, holography and applications to condensed matter arXiv:1610.02681

[44] Burikham P and Poovuttikul N 2016 Shear viscosity in holography and effective theory of transport without translational symmetry *Phys. Rev.* D **94** 106001

[45] Liu H-S, Lu H and Pope C N 2016 Magnetically-charged black branes and viscosity/entropy ratios *J. High Energy Phys.* JHEP12(2016)097

[46] Ling Y, Xian Z-Y and Zhou Z 2016 Holographic shear viscosity in hyperscaling violating theories without translational invariance *J. High Energy Phys.* JHEP11(2016)007

[47] Hartnoll S A, Ramirez D M and Santos J E 2016 Entropy production, viscosity bounds and bumpy black holes *J. High Energy Phys.* JHEP03(2016)170

[48] Alberte L, Baggioli M and Pujolas O 2016 Viscosity bound violation in holographic solids and the viscoelastic response *J. High Energy Phys.* JHEP07(2016)074

[49] Ling Y, Xian Z and Zhou Z 2017 Power law of shear viscosity in Einstein–Maxwell-dilaton-axion model *Chin. Phys.* C **41** 023104

[50] Cisterna A, Hassaine M, Oliva J and Rinaldi M 2017 Axionic black branes in the *k*-essence sector of the Horndeski model *Phys. Rev.* D **96** 124033

[51] Baggioli M and Buchel A 2019 Holographic viscoelastic hydrodynamics *J. High Energy Phys.* JHEP03(2019)146

[52] Andrade T, Baggioli M and Pujolàs O 2019 Linear viscoelastic dynamics in holography *Phys. Rev.* D **100** 106014

[53] Zhou Y-T, Kuang X-M, Li Y-Z and Wu J-P 2020 Holographic subregion complexity under a thermal quench in an Einstein–Maxwell-axion theory with momentum relaxation *Phys. Rev.* D **101** 106024

[54] Baggioli M and Li W-J 2020 Universal bounds on transport in holographic systems with broken translations *SciPost Phys.* **9** 007

[55] Wang X-J and Li W-J 2021 Holographic phonons by gauge-axion coupling *J. High Energy Phys.* JHEP07(2021)131

[56] Baggioli M, Li L and Sun H-T 2022 Shear flows in far-from-equilibrium strongly coupled fluids *Phys. Rev. Lett.* **129** 011602

[57] Xia L-Z and Li W-J 2024 Hydrodynamic modes in holographic multiple-axion model *Eur. Phys. J.* C **84** 1236

[58] Baggioli M, Cremonini S, Early L, Li L and Sun H-T 2023 Breaking rotations without violating the KSS viscosity bound *J. High Energy Phys.* JHEP07(2023)016

[59] Baggioli M and Pujolas O 2015 Electron-phonon interactions, metal-insulator transitions, and holographic massive gravity *Phys. Rev. Lett.* **114** 251602

[60] Alberte L, Baggioli M, Khmelnitsky A and Pujolas O 2016 Solid holography and massive gravity *J. High Energy Phys.* JHEP02(2016)114

[61] Baggioli M, Kim K-Y, Li L and Li W-J 2021 Holographic axion model: a simple gravitational tool for quantum matter *Sci. China Phys. Mech. Astron.* **64** 270001

[62] Baggioli M, Li L, Li W-J and Sun H-T 2024 Mechanical stability of homogeneous holographic solids under finite shear strain *J. High Energy Phys.* JHEP05(2024)198

[63] Alberte L, Ammon M, Jiménez-Alba A, Baggioli M and Pujolàs O 2018 Holographic phonons *Phys. Rev. Lett.* **120** 171602

[64] Baggioli M and Grieninger S 2019 Zoology of solid & fluid holography—Goldstone modes and phase relaxation *J. High Energy Phys.* **2019** JHEP10(2019)235

[65] Ammon M, Baggioli M and Jiménez-Alba A 2019 A unified description of translational symmetry breaking in holography *J. High Energy Phys.* JHEP09(2019)124

[66] Alberte L, Baggioli M, Castillo V C and Pujolas O 2019 Elasticity bounds from effective field theory *Phys. Rev.* D **100** 065015

[67] Delacrétaz L V, Goutéraux B, Hartnoll S A and Karlsson A 2017 Theory of hydrodynamic transport in fluctuating electronic charge density wave states *Phys. Rev.* B **96** 195128